Eur. Phys. J. Spec. Top. (2022) 231:4221–4232
https://doi.org/10.1140/epjs/s11734-022-00569-8

THE EUROPEAN PHYSICAL JOURNAL SPECIAL TOPICS

Review

Materials under extreme pressure: combining theoretical and experimental techniques

Bhargavi Koneru[1], Jhilmil Swapnalin[1], P. Banerjee[1,a], Kadiyala Chandra Babu Naidu[2], and N. Suresh Kumar[3]

[1] Multiferroic and Magnetic Material Research Laboratory, Gandhi Institute of Technology and Management (GITAM) University, Bengaluru, Karnataka, India
[2] Department of Physics, Gandhi Institute of Technology and Management (GITAM) University, Bengaluru, Karnataka, India
[3] Department of Physics, JNTUCEA, Anantapuramu, AP, India

Received 5 November 2021 / Accepted 9 April 2022 / Published online 18 April 2022

Abstract The application of high pressure during the synthesis of materials has a substantial impact on the properties and yield of materials. These can further make the electron more energetic for efficient hybridization. Ultimately results in unprecedented bonding, unusual stoichiometry and properties. Recent advancement computing with the first principle technique makes it possible to predict the existence of these materials under extreme pressure with simulations. The main challenge associated with exotic chemical materials is their instability at room temperatures after the release of pressure. In this work, we tried to address this problem with a greater highlight on a wide range of materials under extreme pressure and their future outlook.

1 Introduction

Material scientists employ diverse methods of synthesis to prepare the different materials, which show diverse properties. Particularly, the effect of pressure during the synthesis of materials has a great impact on the yield and properties of certain materials. The pressure scale of the earth surface to core ranges from 10^{-4} to 360 GPa. Whereas the sun has 2.6×10^7 GPa pressure at the core and the biggest planet Jupiter has 400 GPa [1]. Regardless of this huge pressure, scales of the synthesis of materials can be done at normal temperature.

For generations, people have been behind high-pressure synthesis due to its ability to synthesize rare and expensive elements like diamond and other superconducting and super hard materials, which have immense application. When the external high pressure is applied to these molecular compounds, phase transformation is expected. Due to that, the electrons inside the intermolecular bonds delocalize to form polymeric solids [2]. The ammonia material belongs to the group of archetypal binary compounds that occurs abundantly in major giant gas planets like Uranus, Neptune and in many solar planets. The rare phenomenon of transforming a solid molecule into an ionic solid is a difficult task, whereas the high-pressure compression makes it very simple. Ammonia is said to be superionic at 90 GPa at certain high-temperature conditions. In ammonia, the hydrogen molecules inside it undergo rapid hoping to form a stable superionic solid and act as a protonic conductor. When ammonia is subjected to high pressure, it condenses due to the compression of intermolecular spaces. The hydrogen bonds become more distorted and very weak. In crystalline ammonia, when pressure is applied to ammonia at around 100 GPa, hydrogen bonds evolve periodically to form a solid symmetric hydrogen bond. But the solid ammonia is thermodynamically unstable at low temperatures till 300 GPa. Ammonia also exhibits a superionic state at 150 GPa compression and is stable till 110 GPa on decompression [3]. Applying pressure is a plain sailing way to convert any material into a crystalline structure. Due to compression and high pressure, the material shows different phase transformations, unique electronic configurations, and some elements exhibit superconductivity at some high pressure.

At high pressure, many elements exhibit superconductivity. Elements like neon, xenon and some other elements like nitrogen transform to a metallic state. The hydrogen also attracts more attention as it is very difficult to treat under high-pressure conditions. Despite these ambiences, the hydrogen atom is subjected to the pressure of 140 GPa at that stage, hydrogen transforms into a metallic fluid. It shows different optical properties, which happens due to the decrease in the energy gap between the bands and increase in the electron density [4].

A decrease in interatomic distances inside the materials under pressure may lead to an increase in the width of the conduction and valence bands. For instance,

[a] e-mail: pbanerje@gitam.edu (corresponding author)

sodium becomes optically transparent under pressure 200 GPa. It becomes dielectric with increasing the energy gap and monatomic in nature where valence electrons exhibit high energy with an increase in the pressure [5]. The transition of metals to semiconductors occurs due to induced high pressure. Metals like Li exhibit complex behaviour with different pressure scales with respect to ambient conditions' simple BCC structure, whereas with an increase in pressure, Li changes its cubic structure to an intermediate FCC structure. At 70 GPa, the lattice structure of Li is Rhombohedral, and lattice structure changes to Orthorhombic at 269 GPa due to an increase in the compression and effect of localization charges at interstitial sites [6].

The chemical identity of materials also plays an important under compression. The elements from the periodic table of different groups show different chemical changes under pressure. With a few d-block elements, the chemical hardness increases with pressure. It is due to their spin polarization of elements and half-filled shells. In contrast, the f-block elements cannot be treated above 500 GPa because of their smaller eV and zero electron affinity. The elements with good electronegativity will show greater chemical identity. In most of the elements, electronegativity will increase initially and then decrease. Due to pressure, the change in atomic properties occurs because of an increase in kinetic energy, electron–nuclear attraction and core-valence repulsion [7].

Hence, the materials synthesized with high pressure play an important role as they are modified according to the need for better application. In this process, the materials undergo size, shape and properties modification. In general, the materials synthesized under high compression can be broadly classified into he following four categories: They are exotic, superhard, superconductive, and energy materials. The materials under extreme pressure possess an unique chemical identity. Variable thermal properties, greater electrical conduction, increased durability, better oxidation properties make materials under extreme pressure more specialized and also have a wide range of industrial applications like marine, aerospace, oil and gas extraction and many others [8]. With all these properties and applications, materials under extreme pressure are more prominently used in the domain of materials technology. Hence, in this review we focus on the recent development in the field of materials under extreme pressure.

2 Experimental tools available to generate high compressions

Experimental tools available to generate high compressions are basically of two types, Static and Dynamics compression methods. Both these methods are complementary to each other in extreme conditions. Present-day researchers can study materials under extreme conditions with different techniques by generating compression statically or dynamically.

2.1 Static

2.1.1 Double-stage diamond anvil cell

The diamond anvil cell method provided static compression of 400 GPa at room temperature to study the materials in extreme pressure. A new technique, known as the ds-DAC (double-stage diamond anvil cell), was developed in 2012 [9]. This breakthrough made it possible to obtain 600 GPa static pressure above the typical DAC limit. This paper showed a new combined approach to gain more static pressure. Authors used "Nano-crystalline diamond," i.e., NCD micro-semi-balls synthesized directly from glassy carbon balls as a second stage anvil in the conventional DAC. ds-DAC was proven to be advantageous over DAC as the restricted compression generated strengthens the second stage anvils.

Dubrovinsky et al., after performing countless experiments on the new second-stage anvils, documented their particular observations. It reflects the following: (1) when it placed on the primary, may slightly change its position due to high compression, leading to distorted alignment with a drilled small cavity on the surface. (2) if the secondary anvils get interposed below 30–35 GPa between the primary anvils, the NCD have chances of gliding over each other, which degrades the lower limit of compression achievable at that moment. (3) Misalignment can also happen if the sample size is bigger than the anvils [9]. None other succeeded in generating such high-value static compression while the same group reported achieving 750 GPa by studying the most incompressible metal Osmium under static pressure [10].

Sakai et al. tried to use this ds-DAC technique to generate high compression by fabricating focused ion beam micron-sized diamond anvils to address the experimental complexities. They made the micron-sized second-stage anvils from single crystal and polycrystalline diamond by carving out the pair from one block of material. With platinum foil in the middle of culets, they were fitted in the centre using the Rhenium gasket and Glycerin as the pressure medium. They could achieve a pressure of around 300 GPa, showing that micro anvils' misalignment is solvable by the fabrication [11]. They again reported their observations by making two micro anvils separately and assembling them with a GC rod. They placed a disk-like rhenium sample in culets of micro-anvils. They performed about 13 various ds-DAC experiments by changing the sample or micro-anvils type and position and could achieve pressure between 430 and 450 GPa utmost [12].

A new support system, known as conical support, was proposed in 2019 to strengthen the second-stage anvil. The ideal shape and set up of both conical ds-DAC and toroidal DAC is identical [13,14]. Microanvils were made of ultra-fine nano-polycrystalline diamonds

(NPD) and fabricated in a lozenge-like shape. In the first-stage anvil, a cavity was made to fit micro-anvil by depositing platinum. It was only possible to get compression of about 500 GPa. Further, they used NPD to make both first- and second-stage anvils and could record the pressure of 300 GPa [15]. Despite many other groups' failures, the same group achieved compression in the range of Terapascal by using transparent nanodiamond micro balls as secondary anvils, this time with an internal gasket attached to the setup paving a new way to use liquid and gaseous samples between the anvils [16].

2.1.2 Piston–cylinder devices

The apparatus comprises a blind hole in a piston of circular cross-section sliding to provide quasi-hydrostatic compression to the sample. The maximum compression generation is limited by the piston's crushing strength [17]. In the 1960s, Piston–cylinder devices were widely used for phase-equilibrium studies at high temperatures and pressure. Boyd and England showed hydrostatic pressure conditions were well achieved in this apparatus compared to the anvil apparatus. Though the pressure generated is less than an anvil set-up, it gives high precision in pressure measurement [18]. Still, there are chances of pressure loss due to friction, medium, and walls of pressure vessel and for inherent effects present in the pressure medium [19]. Pressure calibration was done to study the effect of friction using two pressure mediums, talc and silver chloride, at high-compression temperature conditions [20].

In the high-compression realm, to fix the compression of the Ba I–II transitions as the calibration point, a piston–cylinder apparatus with single-stage was used to record the pressure [21]. When crystalline and glassy materials were compressed under piston–cylinder, they always cracked during compression, decompression, and quenching. Uncracked quartz crystal was achieved by slow compression and decompression at about 1.5 GPa [22] and using the water-filled canisters [23,24]. The uncracked single-crystal olivine from 2.0 to 3.0 GPa at 1000–1600 °C was obtained using piston–cylinder apparatus to extend this work, [25]. Then a piston–cylinder apparatus with two movable pistons coated with electrically insulating material was invented to produce diamond crystals, thereby maintaining a pressure of around 20 Kb. In the subsequent year, a simple piston–cylinder model was developed, which aided the synthesis of high Tc superconductors, new crystalline materials with a maximum pressure of 10 Kbar and 1200 °C. The compounds that attain superconductivity at only high pressure can be stabilized by simultaneously applying high pressure and temperature.

The piston–cylinder is best suited compared to other apparatus [26]. An assembly with a soft medium and internal heater of 1400 K capable of achieving compression of 3 GPa termed as gas piston–cylinder is a new approach to reduce experimental uncertainty in pressure scale [27]. Phase transition study of MnSi crystal at high compression was triggered with liquid pressure medium by a piston–cylinder apparatus to study the critical quantum region at high compression and low temperature [28]. In 2017, a double-walled piston–cylinder with low background, favorable for μSR experiments was developed which could reach about 2.2 GPa at low temperature and about 2.6 GPa at normal room temperature [29]. The piston–cylinder technique is used for compression of more than 10 K bar, a range difficult to access by most gas-pressure apparatus, and is also suitable for low-pressure experiments [30]. This device's merits are faster quench rates, a simple sample assembly setup, and low maintenance cost compared to other apparatuses.

2.2 Dynamic

2.2.1 Shock wave with a gas gun

Dynamic compression can be achieved by producing shock waves using a gas gun. The underlying principle is applying a strong force on the sample and determining its consequences with other special techniques. It is evident that this method gives higher compression and temperature than its static counterpart. It can generate 500 GPa in hydrogen and 50,000 K temperature when compared with conventional DAC in static compression, which goes up to ∼320 GPa at a very low temperatures. In 1966, a group of researchers used a light gas gun of 20 mm to strike onto a target plate with high velocity to produce shock waves, hence creating a high-pressure region. They achieved shock waves in multi mega bars and studied materials properties at high-pressure conditions [31].

In shock dynamics experiments, the gas gun is widely used for its advantages like precise compression generation with well-defined projectile and target, adequate and controlled impact velocity range, easy operation with only a few personnel, facilitates temperature variation in the sample, uniform and one-dimensional Shock wave flow can be produced [32,33]. The two-stage light gas gun produced instant, irreversible shock waves of 20 to s 500 GPa facilitating studies of matter at extreme conditions [34]. In later years, the lab enabled the successful measurement of the Hugoniot point of Sapphire, an important window for material in high compression [35]. A compressed gas gun was used in water to produce a steady and plane shock wave up to 1 GPa to study the shock Hugoniot compression curve of liquids [36]. Due to short-time operation, Underwater Shock waves were also proved to be beneficial to bond directly multi-metals stacked in multilayer to fabricate graded density impactor with reduced anomalies in the matter [37].

2.2.2 Shock wave with laser

Shock waves can be procured easily by using the laser as an illuminating source giving high-amplitude waves at a short time with a high repetition rate. These

Table 1 Progress of exotic chemical materials with high compression force

Material	Compression force (GPa)	Contribution
Hydrogenated–C	25	By modifying the solid state synthesis reaction at high compression and temperature, the basic structure of crystal of the benzene molecules transform into the hydrogenated–C by breaking the C–C bonds at a pressure of 25 GPa at this temperature, amorphization of benzene happen to create the hydrogenated–C [45]
NO^+ and NO^{3-}	21	At standard pressure, the NO_2 molecule exits as Polaroid with larger molecules, whereas it transforms into an ionic solid at high pressure (∼21 GPa). The charge interaction depends on the pressure given and alien in the possible coupled orientations forming stable solid molecules of NO^+ and NO^{3-}. This high pressure forms an ionic phase with more excellent dielectric properties [46]
C_2N_2 (NH)	41	DCDA (dicyandiamide) in an anvil heated and subjected to high compression. This resulted in the formation of single crystals of N and C with a ratio of 3:2, and also, the presence of hydrogen was observed forming the single crystal C_2N_2 (NH) compound [47]
Electride Li	80	Lithium is a soft metal when treated at ∼80 GPa pressure; it acquires a low-symmetry structure. With the increase in pressure, Li's resistivity also increases and becomes electrically resistive. It also transmits as a pressure-induced metal to semiconductors [48]
Electride Na	200	Under high pressure, sodium changes its cubic structure from body centre to face centre acquiring the monoatomic state at 60 GPa pressure. Yanming Ma et al. mainly explained the transparency of the material at high pressure; at pressure 200 GPa, sodium changes its form and appears optically transparent with the band gap of eV [48]

special characteristics make laser-shocks different from conventional shock wave production with high chances of shocking samples recovery [38]. Lasers accurately change the pressure level, and temporal pulse profile of the shock transferred to the material [39]. In 1967, Landt and Bell came up with an experiment to study the liquids at extreme dynamic pressure conditions using a Q-switched laser and obtained high-pressure shock waves at pressure ∼200 Kbars [40]. High-energy short-duration laser beam pulses produce high-amplitude shock waves capable of altering the material properties. When combined with transparent overlays, it is reported to generate pressure pulses of 6–10 GPa [41].

It is also possible to measure absolute Hugoniot point in dynamic pressure at multi mega bar scale to derive the equation of state [42]. By passing laser-induced shock waves through the samples pre compressed in a diamond-anvil cell is a combination of static and dynamic type of compression which can generate pressure at tera pascal range (10−100 TPa) [43]. Unlike conventional ways, it offers many advantageous techniques to study the phase transitions like direct laser drive, spallation, equation of state, quasi-isentropic loading, shock recovery, XRD and spectroscopy [44].

3 Progress of exotic chemical materials with high compression force

We can broadly classify the available exotic chemical materials synthesized under a high-compression force of three types, namely electrides, materials with unprecedented ionic bonding, and materials with unusual properties and stoichiometric. The progress of the work so far in the field of exotic chemical materials synthesized under high compression force is highlighted in Table 1.

3.1 Electride

This special classes of exotic chemical materials have excess electrons trapped under lattice voids. These trapped electrons act as anions, whereas ionic solids act as cations. The application of the high-compression force led to the bonding between the anions and cations, which led to the formation of the electrides.

3.1.1 Transparent electride phase of Na

Sodium exists in a wide variety of forms with chlorides and hydroxides. In a diatomic state at ambient conditions, sodium adopts the simple body centred cubic (BCC) structure. When specific temperature and pressure is applied to Na, it starts changing its properties by breaking the alkali bonds and adopting a low symmetric structure and transmit into a metal-insulator. Under high pressure, sodium changes its cubic structure from

body centre to face centre acquiring the monoatomic state at 60 GPa pressure.

Yanming Ma et al. mainly explained the transparency of the material at high pressure; at pressure 200 GPa, sodium changes its form and appears optically transparent with the band gap of eV. It is also clear that at high pressure, sodium acts as an insulator. In contrast, with high compression, sodium undergoes property change due to heavy compression, the atoms inside the sodium overlap. It forces the outermost electrons to holes, resulting in the breakage of the metallic state of sodium. This leads to the energy drop in the 3d band analogized to 3p, showing hybridization loss which is directly proportional to core–core overlap or core–valence overlap. D.H.C.P. (Double hexagonal close packing) structure of Na was revealed by DFT simulation at high pressure of 1000 GPa at this point; the sodium electride exhibits a minimal c/a ratio compared to the native ratio, and the atoms in this phase possess the sixfold coordination indicating the formation of new structure type. The experimental and theoretical studies revealed that sodium at high pressure undergoes phase change at 200 GPa, transforming into a transparent material with a wide bandgap and simulation at 1000 GPa revealed the new double hexagonal closed packing structure of the material [49]. The isocontour plots and absorption spectra are shown in Fig. 1 [50]. It clearly demonstrates that at lower energies, the strength of the optical oscillators redistributed itself. The narrowing of the peak is also visible at around 5 eV with bound excitations.

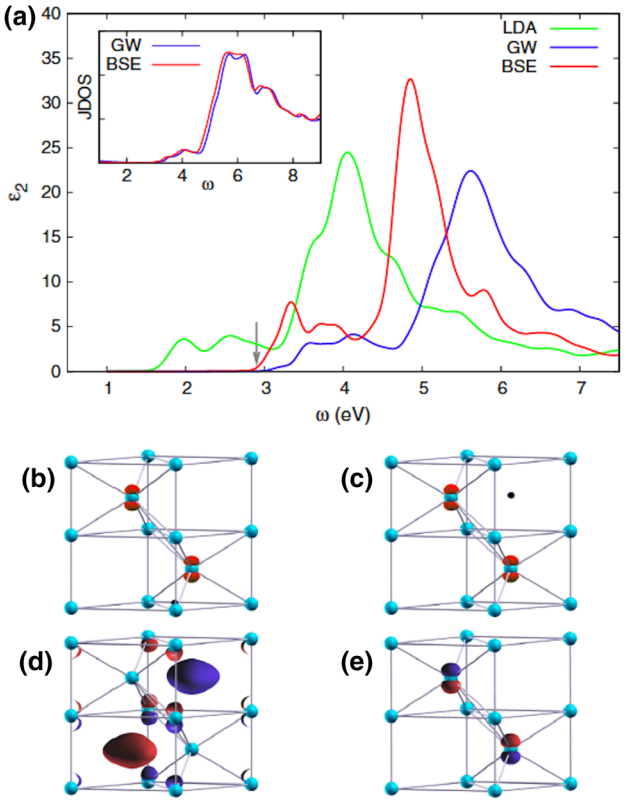

Fig. 1 **a** Absorption spectra, **b**, **c** isocontour plot, **d** Kohn Sham top valence and **e** wave function at the bottom of conduction in dense sodium [50]

3.1.2 Semiconducting electride phase of Li

free electron model of Lithium describes the electronic properties and explains its nearly free electron structure and model. With the well-defined electronic structure of the free electron model, the electronic properties and the electride phase of Lithium is described; however, at high pressure, the Pre electronic structure of Lithium breaks down, and the electronic properties change. This also helps us to identify the pseudogap openings and the change in the Fermi surface. All the changes are observed at high compression [51]. A metal to semiconductor shift of Li is observed, which leads to the formation of dense Lithium. The alkali lithium adopts a simple BCC structure at normal conditions with no pressure or compression, whereas at 42 GPa, Lithium changes its structure from superficial BCC to Complex cubic structure with intermediate fcc and rhombohedral structure change, and this structure is stable up to ∼70 GPa. Lv et al. have studied the properties of Lithium at different pressure scales with the new particle Swarm Optimization algorithm technique, which gives the crystal structure of the metal. Through this technique, the found that the metal lithium exhibits Aba2-40 structure with staggered layers at 60–80 GPa, also at 185–269, GPa reveals the orthorhombic structure. One might expect Lithium to display zero point energy because of its low atomic number. Indeed it shows 87 meV/atom at 70 GPa pressure with the Aba2-40 structure, but this does not affect its structural order. The interatomic distance between the two lithium atoms is 0.161 nm at high pressure; the distance between two atoms decreases, showing a minimum of 0.076 nm at 70 GPa. This signifies the stable valence electrons that induce physical properties to change, like metal to semiconductor transmission. The calculated values of the enthalpies of different structures are shown in Fig. 2 [6]. It can be clearly visible from the figure that Aba2-40 is mainly favorable beyond the 60 GPa than the $I\bar{4}3d$ structure.

3.1.3 Electrides phase of Mg

The electride phase of high-pressure magnesium is determined by PSO (particle Swarm Optimisation) algorithm. The general structure of magnesium is identified as a simple HCP, or FCC structure. When magnesium is treated under high pressure, the general crystal structure will change, showing unusual properties and different structures. The computational approach that is the Particle Swarm Optimisation technique helps to identify the special structure of magnesium at different pressures scales. The symmetry of the magnesium at 456–756 GPa is both face-centred cubic (fcc) and simple hexagonal symmetries. Magnesium under high pressure shows electron pair repulsion inside the lattice where the strong valence overlap occurs. Due to this, the dis-

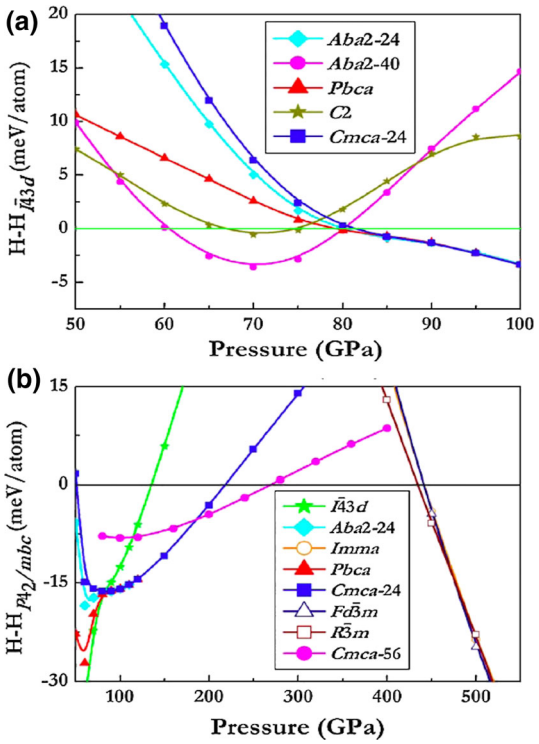

Fig. 2 **a** Enthalpies w.r.t. $I\bar{4}3d$ and **b** $P4_2$/mbc structure of Li [6]

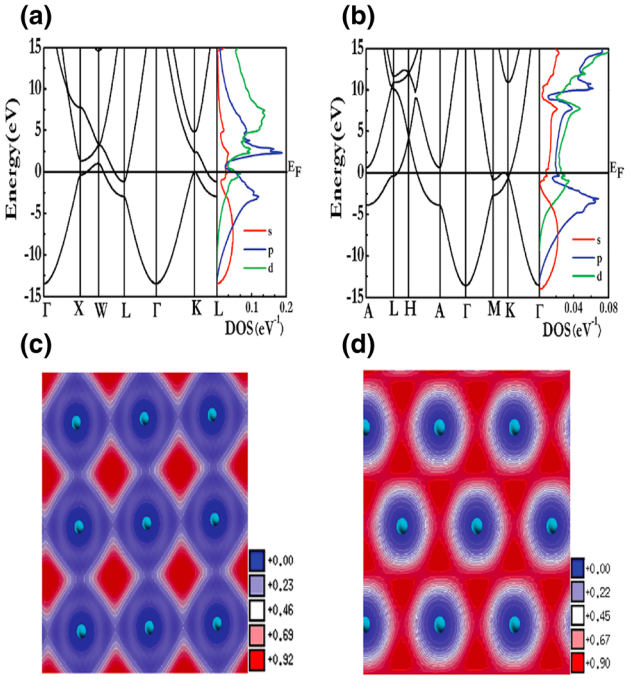

Fig. 3 Band structure of Mg at **a** 500, **b** 800, **c** ELF 500 and **d** ELF 800 GPa pressure [52]

tance between two magnesium atoms changes accordingly with the applied pressure through PSO technique. It is observed that the nearest distance between two magnesium atoms is 0.2094 nm at 500 GPa and 0.1707 nm at 800 GPa. This picture is the transformation of magnesium into a strong electrolyte with greater pressure applied. The band structure calculations of Mg are shown in Fig. 3 [52]. It presents the uniqueness of the fcc-Mg structure with metallic nature. The localization of the valence electrons at the interstitial leads to 0.92 of ELF values.

3.1.4 Mg_3O_2: compound electride

Magnesium oxide is the most abundant alkaline earth metal with different crystal structures predictions. Magnesium oxide is also available in two other most extraordinary compounds like MgO_2 and Mg_3O_2. Magnesium oxide is the most stable element under high pressure. It can withstand pressure and compression up to 850 GPa. At this pressure range, it also produces two different compounds MgO_2 and Mg_3O_2, with more excellent thermodynamic stability. MgO_2 reveals the charge transfer in magnesium oxide with the peroxide ions presence with not much pressure variations, whereas Mg_3O_2 at a pressure of 500 GPa incident enormous property changes with principal thermal stability. Electron localization function theory offers the information of valence electron configuration and bonding character through this method. It is identified that the initial distance between two magnesium atoms is 0.2 nm with pressure, the magnesium atom undergoes core valency explosion, and at this point, there is a change in the electronic configuration of magnesium and also covalent bond breakages with different valency shell atoms of magnesium and giving the new compound Mg_3O_2. The electronic localization and solid covalent bonding between two magnesium atoms result in the anion deficient compound Mg_3O_2 at a pressure range of 500 GPa [53].

3.2 Materials with unprecedented ionic bonding

The application of the hig-compressive force also led to the distribution of charges. These led to the formation of unprecedented ionic bonding that gave rise to another class of exotic chemical materials.

3.2.1 $NO^+NO_3^-$

N_2O is isoelectronic and asymmetric to CO_2 molecules. The polymorphism at high temperature and pressure conditions revealed that N_2O breaks down to the ionic phase. In symmetric piston–cylinder DAC the sample was loaded below 150 K under dry N_2 atmosphere maintained in a glove bag. The sample was exposed by laser at 2000 K, producing high compression and temperature within 10–30 GPa range. A new phase formation was observed. Observing the N_2 and $NONO_3$ vibrational modes, the reaction involving $4N_2O$ was proposed, giving $NONO_3$ and $3N_2$ as by-products in a photochemical transformation. The product obtained when analyzed through Raman, IR spectroscopy with X-ray diffraction data revealed the increase in ionic charac-

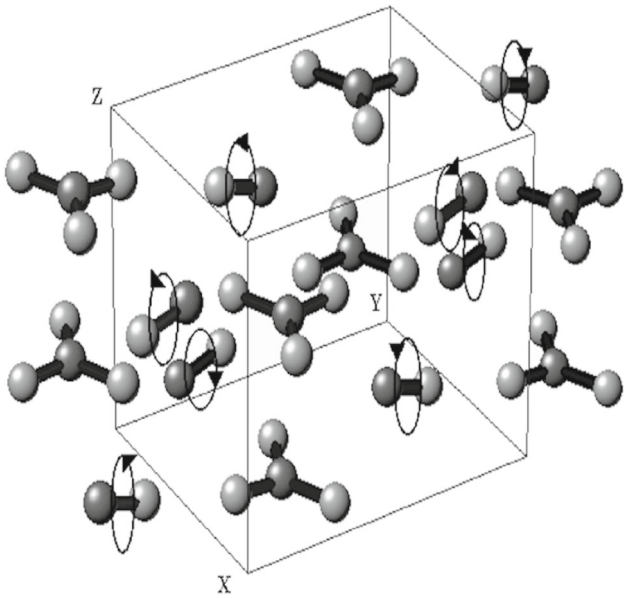

Fig. 4 Structure of high pressure $NONO_3$ [46]

teristics in the solid. It showed that the structure of $NONO_3$ is like an ionic crystal solid of aragonite type shown in Fig. 4. The study showed how at the low-pressure range comprising N_2O_4, the material is molecular in nature, while on increment in pressure due to charge transfer, it turns out to be an ordered ionic solid. Hence, there is a possible area to explore with the ionic phase at this high-temperature–pressure condition exhibiting interesting electronic properties [46].

3.2.2 Highly compressed ammonia forms

Ammonia (NH_3), existing under a wide range of temperature and pressure, is found significantly in the planets and their satellites and extra-solar planets [54]. The ice layers at the core of Neptune and Uranus, composed of water, ammonia, and methane, are present under a pressure 20–600 GPa and ranging from 2000 to 7000 K temperature [55,56]. The computational simulations using first-principles DFT calculations via LDA and GGA, particularly the crystallographic study of NH_3, were predicted under extreme compression. Ammonia, a well-known hydrogen-bonded molecular compound [57] with weaker H-bonds (as compared to water) predicted to form ammonium amide when applied high pressure (∼90 GPa). It forms an ionic solid with alternate NH^{4+} and NH^{2-} ion layers and is reproducible in the laboratory environment. {Experimentally studied only up to 350 GPa, NH_3 was studied at 440 GPa, showing the transition from ionic phase to orthorhombic symmetry. And it noted that high pressure of up to ∼500 GPa and low temperature and NH_3 is found insulating and ready to decompose into N_2 and H_2 [58]. This ionic phase formation was supported later by a joint investigation using experimental and theoretical tools conducted by a group of researchers. High compression

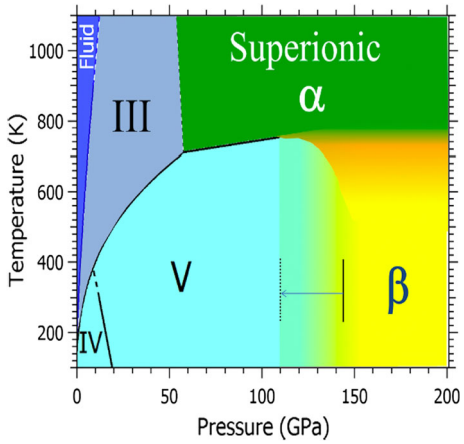

Fig. 5 Phase diagram of NH_3 [3]

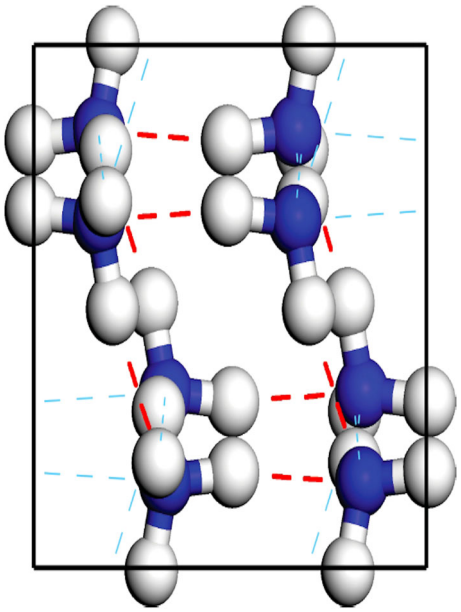

Fig. 6 The structure of the mixtures of ammonia and water at 5 GPa [59]

using the Diamond-anvil technique was applied to both NH_3 and ND_3 at 194 and 184 GPa. A thorough experimental investigation was done using XRD analysis, Raman scattering, IR-absorption spectroscopy. Various possible structures were predicted theoretically using DFT calculations. The phase transition was observed at ∼150 GPa with a structure made up of ionic species shown in Fig. 5 [3]. The experimental and theoretical evaluation led to the information that the formation of NH^{4+} and NH^{2-} is due to the proton-transfer within the molecules under high pressure, forming the ionic state. Furthermore, proton transfer being continuous and reversible induces auto-ionization in the molecular NH_3 at 120 GPa and completes the process at ∼125 GPa [2].

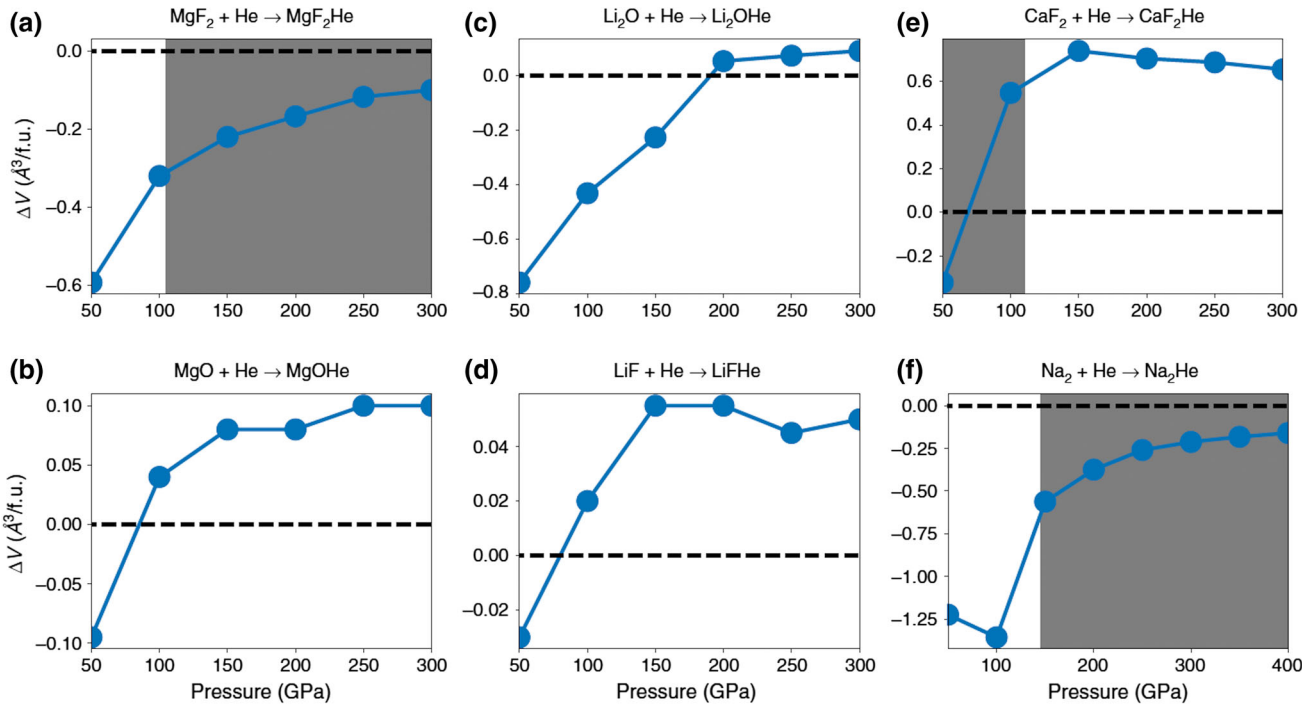

Fig. 7 PV diagram of the exotic materials with unusual stoichiometries for **a** MgF_2He, **b** MgOHe, **c** Li_2OHe, **d** LiFHe, **e** CaF_2He, and **f** Na_2He [67]

3.2.3 Highly compressed water forms

In the core of many giant planets, condensed water ice is found. It is a member of archetypal binary compounds [60,61]. So the study of the ice is significant in examining the nature of the planetary core and helpful in understanding their magnetic field distribution [62,63]. It is verified experimentally, at high pressure above 70 GPa and low temperature, ice breaks in the forms of a stable crystalline phase, i.e., X phase, consisting of O atoms bonded to 4 H atoms via symmetrical hydrogen bonds. At extreme temperature and pressure conditions, ice attains a superionic state [56,64], where the hydrogen atom diffuses due to O–H bond breakage while the Oxygen stays fixed in the lattice. In contrast, the covalent bond between H–O does not break at the low-temperature condition, and H transfer between 2 water molecules is nearly impossible due to the considerable energy cost in solid. In the present decade, a new prediction has come up employing PSO algorithm used to study structure at 0 K and 14 Mbar compression. The crystal structure was analyzed using CALYPSO, and two new ice phases were predicted, one of which is the monoclinic P21 structure, which showed a very interesting ionic state comprising alternate hydroxide (OH^-) and hydronium (H_3O^+) ions. The P21 structure is found to be dynamically stable and favourable to exist at a higher pressure range like 16–20 Mbar. Deep analysis of chemical bondings was performed by calculating electron localization functions (ELF), which confirmed the formation of hydroxide and hydronium ions covalently coupled with a small charge distribution. Bader's quantum theory, when applied was found to be in agreement with the ELF study. It was noted that the ionic charge distribution between two ions is about 0.62 and given as $(H_3O)^{\delta+}$ and $(OH)^{\delta-}$ ($\delta = 0.62$). Using DFT, it was inferred that metallization of water ice at low-temperature is possible when pressure applied is relatively high [65].

3.2.4 Highly compressed ammonia and water conjugate forms

The Interior of Neptune and Uranus is filled with "hot ices" comprising hydrocarbons, water, and ammonia at definite proportion [55]. These ice layers are explored in order to know more about the properties of planets like gravitational moment, magnetic field origin, atmospheric condition, and composition. The behavioural data of the ice at extreme conditions are well documented through the shock wave experiment. Out of the three components present, water is present at a more significant proportion and is thought to be the source of high conductivity due to its ionization [66]. A group of researchers performed calculations to document the phase diagrams of water (H_2O) and ammonia (NH_3) within 30–300 GPa pressure and temperature range within 300 to 7000 K. It was noted that the water and ammonia conjugate achieves an ionic state and behaves electronically as an insulating fluid. It was known earlier that the core of the planet is at 7000 K and 600 GPa, predicted as an ideal condition where water and ammonia could be considered to be metallic. Possibly, at this extreme condition, H_2O shifts from its fluid phase to

metallic at exceeding 7000 K and NH_3 at 5500 K [56]. And under extreme compression, the mixtures of water and ammonia were transformed into ionic solids of the ammonium hydroxide structure shown in Fig. 6 [59]. Here the hydrogen bonding represented with the dashed line with nitrogen and hydrogen atoms is with blue and white spheres, respectively.

3.3 Material with unusual property and stoichiometry

High compression also makes it possible to alter the chemical reaction barrier between the elements. These fundamentally can modify the identity of the compound completely and show some unusual properties. For example, it was believed that the noble gases (NGs) did not react with any other elements due to their completely filled orbits. But the application of the high-compression force can help the NGs chemically react to the other elements. These led to the new class of exotic chemical materials which are having unusual stoichiometry, and that led to their unusual properties as well. In most such applications, the high compression led to the oxidation state of NGs. These help them to share their completely filled electrons with other elements with the formation of chemical bonds.

Recently, it was revealed that when the NGs come in contact with alkali ions with high-compression forces, they gain electrons, e.g. Xe_2F. Even the role of the high-compression force can also form chemical bonding between the NGs with other completely filled orbits such as hydrogen and nitrogen gases. These led the unusual stoichiometries such as Xe–N_2 and Xe–H_2. In general, reported literature indicates Kr, Xeand Ar NGs to be greater reactivity under high-compression conditions. But, the favourable reaction with He is also possible if we use two different cations and anions AB_2 or A_2B under high compression. At the beginning of the low-pressure conditions, the repulsive force between the cations or anions leaves room for the insertion of the He into the structure. It leads to the higher gain in the PV compression terms shown in Fig. 7. It can be understood that the increase of compression force increases the repulsion and decreases the Madelung energy for the stability of the material.

4 Conclusions

The advancement of computing with first principle techniques makes it possible to predict the existence of chemical materials with unusual stoichiometry, unprecedented bonding, and their properties with simulations. The progress in theory and experimental technologies in the field of high-compression methods realized the synthesis techniques for these exotic chemical materials in real life applications. The progress in both the fields of theory and experimental designs start showing promising applications in the field of materials science of exotic chemical materials.

The main challenge associated with these applications is that high-pressure exotic chemical materials are in general unstable at room temperatures. The approaches to synthesize these high-compression materials had different strategies. One such strategy is to apply high-compression force at high temperature and thereafter fast quenching to room temperature. But these always lead towards the polycrystalline small sized grains. On the other hand, it is also possible to synthesize the exotic chemical materials by bottom-up approach like CVD or MBE. But very few high-pressure chemical materials have been prepared with these techniques within thin film forms. The synthesis techniques of applying high-compression force through nano-structuring also have an alternative way to obtain chemical materials. In any way, the proper knowledge of the phase diagram is very crucial for their stability at the ambient conditions.

A wide range of promising materials shows potential properties at high compressions. But the high-pressure chemical materials with unusual bonding and stoichiometries show the most potential properties at the ambient conditions. Broadly, we can classify these high-pressure exotic chemical materials into three categories such as electrides, materials with unprecedented ionic bonding and materials with unusual properties and stoichiometric.

Although the field of high-pressure chemical materials is extremely rich, we tried to highlight a wide range of high-pressure exotic chemical materials and available techniques to predict them. Variable thermal properties, greater electrical conduction, increased durability and better oxidation properties make these materials more specialized. The high-pressure chemical materials also have applications in marine science, aerospace, oil and gas extractions. The progress in the field of high-pressure chemical materials can open the avenue of greater discoveries and potential opportunities, which is not possible for the materials synthesized at the ambient pressures.

Funding P. Banerjee acknowledges financial helps received from SERB, India as TARE fellowship and TAR/2021/000032 research Grant.

Data availability statement The data will be made immediately available based on the request.

Declarations

Conflict of interest The authors declare that we have no conflicts of interest.

Institutional review board statement Not applicable for studies not involving humans or animals.

Informed consent statement Not applicable for studies not involving humans or animals.

References

1. J.P.S. Walsh, D.E. Freedman, High-pressure synthesis: a new frontier in the search for next-generation intermetallic compounds. Acc. Chem. Res. **51**(6), 1315–1323 (2018)
2. T. Palasyuk, I. Troyan, M. Eremets, V. Drozd, S. Medvedev, P. Zaleski-Ejgierd, E. Magos-Palasyuk, H. Wang, S.A. Bonev, D. Dudenko et al., Ammonia as a case study for the spontaneous ionization of a simple hydrogen-bonded compound. Nat. Commun. **5**(1), 1–7 (2014)
3. S. Ninet, F. Datchi, P. Dumas, M. Mezouar, G. Garbarino, A. Mafety, C.J. Pickard, R.J. Needs, A.M. Saitta, Experimental and theoretical evidence for an ionic crystal of ammonia at high pressure. Phys. Rev. B **89**(17), 174103 (2014)
4. C. Buzea, K. Robbie, Assembling the puzzle of superconducting elements: a review. Supercond. Sci. Technol. **18**(1), R1 (2004)
5. Y. Ma, Y. Li, E. Mikhail, A.R. Oganov, Transparent dense sodium. Wuli **40**(8), 505–509 (2011)
6. J. Lv, Y. Wang, L. Zhu, Y. Ma, Predicted novel high-pressure phases of lithium. Phys. Rev. Lett. **106**(1), 015503 (2011)
7. X. Dong, A.R. Oganov, G. Qian, X.-F. Zhou, Q. Zhu, H.-T. Wang, How do chemical properties of the atoms change under pressure. arXiv preprint arXiv:1503.00230 (2015)
8. R.E. Hummel, *Understanding Materials Science: History, Properties, Applications* (Springer Science & Business Media, Berlin, 2004)
9. L. Dubrovinsky, N. Dubrovinskaia, V.B. Prakapenka, A.M. Abakumov, Implementation of micro-ball nanodiamond anvils for high-pressure studies above 6 mbar. Nat. Commun. **3**(1), 1–7 (2012)
10. L. Dubrovinsky, N. Dubrovinskaia, E. Bykova, M. Bykov, V. Prakapenka, C. Prescher, K. Glazyrin, H.-P. Liermann, M. Hanfland, M. Ekholm et al., The most incompressible metal osmium at static pressures above 750 gigapascals. Nature **525**(7568), 226–229 (2015)
11. T. Sakai, T. Yagi, H. Ohfuji, T. Irifune, Y. Ohishi, N. Hirao, Y. Suzuki, Y. Kuroda, T. Asakawa, T. Kanemura, High-pressure generation using double stage micro-paired diamond anvils shaped by focused ion beam. Rev. Sci. Instrum. **86**(3), 033905 (2015)
12. T. Sakai, T. Yagi, T. Irifune, H. Kadobayashi, N. Hirao, T. Kunimoto, H. Ohfuji, S. Kawaguchi-Imada, Y. Ohishi, S. Tateno et al., High pressure generation using double-stage diamond anvil technique: problems and equations of state of rhenium. High Press. Res. **38**(2), 107–119 (2018)
13. A. Dewaele, P. Loubeyre, F. Occelli, O. Marie, M. Mezouar, Toroidal diamond anvil cell for detailed measurements under extreme static pressures. Nat. Commun. **9**(1), 1–9 (2018)
14. Z.S. Jenei, E.F.O. Bannon, S.T. Weir, H. Cynn, M.J. Lipp, W.J. Evans, Single crystal toroidal diamond anvils for high pressure experiments beyond 5 megabar. Nat. Commun. **9**(1), 1–6 (2018)
15. T. Sakai, T. Yagi, R. Takeda, T. Hamatani, Y. Nakamoto, H. Kadobayashi, H. Mimori, S.I. Kawaguchi, N. Hirao, K. Kuramochi et al., Conical support for double-stage diamond anvil apparatus. High Press. Res. **40**(1), 12–21 (2020)
16. N. Dubrovinskaia, L. Dubrovinsky, N.A. Solopova, A. Abakumov, S. Turner, M. Hanfland, E. Bykova, M. Bykov, C. Prescher, V.B. Prakapenka et al., Terapascal static pressure generation with ultrahigh yield strength nanodiamond. Sci. Adv. **2**(7), e1600341 (2016)
17. L.H. Cohen, W. Klement Jr., G.C. Kennedy, Investigation of phase transformations at elevated temperatures and pressures by differential thermal analysis in piston-cylinder apparatus. J. Phys. Chem. Solids **27**(1), 179–186 (1966)
18. M. Shimada, Measurement of pressure at high temperatures in a piston-cylinder apparatus. Contrib. Geophys. Inst. Kyoto Univ. **11**, 213–229 (1971)
19. P.W. Mirwald, I.C. Getting, G.C. Kennedy, Low-friction cell for piston-cylinder high-pressure apparatus. J. Geophys. Res. **80**(11), 1519–1525 (1975)
20. T.H. Green, A.E. Ringwood, A. Major, Friction effects and pressure calibration in a piston-cylinder apparatus at high pressure and temperature. J. Geophys. Res. **71**(14), 3589–3594 (1966)
21. J.C. Haygarth, I.C. Getting, G.C. Kennedy, Determination of the pressure of the barium i–ii transition with single-stage piston-cylinder apparatus. J. Appl. Phys. **38**(12), 4557–4564 (1967)
22. A.K. Kronenberg, S.H. Kirby, R.D. Aines, G.R. Rossman, Solubility and diffusional uptake of hydrogen in quartz at high water pressures: implications for hydrolytic weakening. J. Geophys. Res. Solid Earth **91**(B12), 12723–12741 (1986)
23. M. Rovetta, J.D. Blacic, R.L. Hervig, J.R. Holloway, Aluminum and hydrogen defects in quartz: enhanced diffusion at high pressure and high f h2. EOS Trans. Am. Geophys. Union **66**, 627 (1987)
24. J. Gerretsen, M.S. Paterson, J. Bitmead, Improved procedures for diffusing water into quartz at high temperature and pressure. EOS Trans. Am. Geophys. Union **66**, 1144 (1985)
25. T.N. Tingle, Retrieval of uncracked single crystals from high pressure in piston-cylinder apparatus. Am. Mineral. **73**(9–10), 1195–1197 (1988)
26. K. Anbukumaran, C. Venkateswaran, N. Victor Jaya, S. Natarajan, Piston-cylinder apparatus for high pressure and high temperature studies, in *AIP Conference Proceedings*, vol. 309. (American Institute of Physics, 1994), p. 1585
27. P.C. Burnley, I.C. Getting, Creating a high temperature environment at high pressure in a gas piston cylinder apparatus. Rev. Sci. Instrum. **83**(1), 014501 (2012)
28. A.E. Petrova, S.M. Stishov, Phase diagram of the itinerant helimagnet MNSI from high-pressure resistivity measurements and the quantum criticality problem. Phys. Rev. B **86**(17), 174407 (2012)
29. Z. Shermadini, R. Khasanov, M. Elender, G. Simutis, Z. Guguchia, K.V. Kamenev, A. Amato, A low-background piston-cylinder-type hybrid high pressure cell for muon-spin rotation/relaxation experiments. High Press. Res. **37**(4), 449–464 (2017)

30. F. Brunet, D. Vielzeuf, The farringtonite/mg 3 (po 4) 2–ii transformation; a new curve for pressure calibration in piston-cylinder apparatus. Eur. J. Mineral. **8**(2), 349–354 (1996)
31. A.H. Jones, W.M. Isbell, C.J. Maiden, Measurement of the very-high-pressure properties of materials using a light-gas gun. J. Appl. Phys. **37**(9), 3493–3499 (1966)
32. G.R. Fowles, G.E. Duvall, J. Asay, P. Bellamy, F. Feistmann, D. Grady, T. Michaels, R. Mitchell, Gas gun for impact studies. Rev. Sci. Instrum. **41**(7), 984–996 (1970)
33. A.V. Pavlenko, S.I. Balabin, O.E. Kozelkov, D.N. Kazakov, A one-stage light-gas gun for studying dynamic properties of structural materials in a range up to 40 gpa. Instrum. Exp. Tech. **56**(4), 482–484 (2013)
34. A.C. Mitchell, W.J. Nellis, Diagnostic system of the lawrence livermore national laboratory two-stage light-gas gun. Rev. Sci. Instrum. **52**(3), 347–359 (1981)
35. D. Erskine, High pressure hugoniot of sapphire, in *AIP Conference Proceedings*, vol. 309. (American Institute of Physics, 1994), p. 141
36. K. Nagayama, Y. Mori, K. Shimada, M. Nakahara, Shock hugoniot compression curve for water up to 1 gpa by using a compressed gas gun. J. Appl. Phys. **91**(1), 476–482 (2002)
37. W. Sun, X. Li, K. Hokamoto, Fabrication of graded density impactor via underwater shock wave and quasi-isentropic compression testing at two-stage gas gun facility. Appl. Phys. A **117**(4), 1941–1946 (2014)
38. M. Boustie, L. Berthe, T. De Rességuier, M. Arrigoni, Laser shock waves: fundamentals and applications, in *1st International Symposium on Laser Ultrasonics: Science, Technology and Applications* (Citeseer, 2008)
39. P. Peyre, L. Berthe, X. Scherpereel, R. Fabbro, E. Bartnicki, Experimental study of laser-driven shock waves in stainless steels. J. Appl. Phys. **84**(11), 5985–5992 (1998)
40. C.E. Bell, J.A. Landt, Laser-induced high-pressure shock waves in water. Appl. Phys. Lett. **10**(2), 46–48 (1967)
41. A.H. Clauer, J.H. Holbrook, B.P. Fairand, Effects of laser induced shock waves on metals. Shock waves and high-strain-rate phenomena in metals (1981), p. 675–702
42. A. Ng, D. Parfeniuk, L. DaSilva, Hugoniot measurements for laser-generated shock waves in aluminum. Phys. Rev. Lett. **54**(24), 2604 (1985)
43. R. Jeanloz, P.M. Celliers, G.W. Collins, J.H. Eggert, K.K.M. Lee, R.S. McWilliams, S. Brygoo, P. Loubeyre, Achieving high-density states through shock-wave loading of precompressed samples. Proc. Natl. Acad. Sci. **104**(22), 9172–9177 (2007)
44. S.N. Luo, D.C. Swift, T.E. Tierney IV., D.L. Paisley, G.A. Kyrala, R.P. Johnson, A.A. Hauer, O. Tschauner, P.D. Asimow, Laser-induced shock waves in condensed matter: some techniques and applications. High Press. Res. **24**(4), 409–422 (2004)
45. L. Ciabini, M. Santoro, F.A. Gorelli, R. Bini, V. Schettino, S. Raugei, Triggering dynamics of the high-pressure benzene amorphization. Nat. Mater. **6**(1), 39–43 (2007)
46. M. Somayazulu, A. Madduri, A.F. Goncharov, O. Tschauner, P.F. McMillan, H. Mao, R.J. Hemley, Novel broken symmetry phase from n 2 o at high pressures and high temperatures. Phys. Rev. Lett. **87**(13), 135504 (2001)
47. E. Horvath-Bordon, R. Riedel, P.F. McMillan, P. Kroll, G. Miehe, P.A. van Aken, A. Zerr, P. Hoppe, O. Shebanova, I. McLaren et al., High-pressure synthesis of crystalline carbon nitride imide, c2n2 (nh). Angewandte Chemie **119**(9), 1498–1502 (2007)
48. T. Matsuoka, K. Shimizu, Direct observation of a pressure-induced metal-to-semiconductor transition in lithium. Nature **458**(7235), 186–189 (2009)
49. Y. Ma, M. Eremets, A.R. Oganov, Y. Xie, I. Trojan, S. Medvedev, A.O. Lyakhov, M. Valle, V. Prakapenka, Transparent dense sodium. Nature **458**(7235), 182–185 (2009)
50. M. Gatti, I.V. Tokatly, A. Rubio, Sodium: a charge-transfer insulator at high pressures. Phys. Rev. Lett. **104**(21), 216404 (2010)
51. M. Marqués, M.I. McMahon, E. Gregoryanz, M. Hanfland, C.L. Guillaume, C.J. Pickard, G.J. Ackland, R.J. Nelmes, Crystal structures of dense lithium: a metal–semiconductor–metal transition. Phys. Rev. Lett. **106**(9), 095502 (2011)
52. P. Li, G. Gao, Y. Wang, Y. Ma, Crystal structures and exotic behavior of magnesium under pressure. J. Phys. Chem. C **114**(49), 21745–21749 (2010)
53. Q. Zhu, A.R. Oganov, A.O. Lyakhov, Novel stable compounds in the mg-o system under high pressure. Phys. Chem. Chem. Phys. **15**(20), 7696–7700 (2013)
54. D.D. Sasselov, Extrasolar planets. Nature **451**(7174), 29–31 (2008)
55. W.B. Hubbard, Interiors of the giant planets. Science **214**(4517), 145–149 (1981)
56. C. Cavazzoni, G.L. Chiarotti, S. Scandolo, E. Tosatti, M. Bernasconi, M. Parrinello, Superionic and metallic states of water and ammonia at giant planet conditions. Science **283**(5398), 44–46 (1999)
57. F. Datchi, S. Ninet, M. Gauthier, A.M. Saitta, B. Canny, F. Decremps, Solid ammonia at high pressure: a single-crystal X-ray diffraction study to 123 gpa. Phys. Rev. B **73**(17), 174111 (2006)
58. C.J. Pickard, R.J. Needs, Highly compressed ammonia forms an ionic crystal. Nat. Mater. **7**(10), 775–779 (2008)
59. G.I.G. Griffiths, R.J. Needs, C.J. Pickard, High-pressure ionic and molecular phases of ammonia within density functional theory. Phys. Rev. B **86**(14), 144102 (2012)
60. T. Guillot, Interiors of giant planets inside and outside the solar system. Science **286**(5437), 72–77 (1999)
61. J.J. Lissauer, Extrasolar planets. Nature **419**(6905), 355–358 (2002)
62. M. French, T.R. Mattsson, N. Nettelmann, R. Redmer, Equation of state and phase diagram of water at ultra-high pressures as in planetary interiors. Phys. Rev. B **79**(5), 054107 (2009)
63. M. French, T.R. Mattsson, R. Redmer, Diffusion and electrical conductivity in water at ultrahigh pressures. Phys. Rev. B **82**(17), 174108 (2010)
64. V. Petrenko, R.W. Whitworth, *Physics of Ice* (Oxford University, Oxford, 2002)
65. Y. Wang, H. Liu, J. Lv, L. Zhu, H. Wang, Y. Ma, High pressure partially ionic phase of water ice. Nat. Commun. **2**(1), 1–5 (2011)
66. W.J. Nellis, D.C. Hamilton, N.C. Holmes, H.B. Radousky, F.H. Ree, A.C. Mitchell, M. Nicol, The nature of the interior of uranus based on studies of plan-

etary ices at high dynamic pressure. Science **240**(4853), 779–781 (1988)
67. Z. Liu, J. Botana, A. Hermann, S. Valdez, E. Zurek, D. Yan, H. Lin, M. Miao, Reactivity of he with ionic compounds under high pressure. Nat. Commun. **9**(1), 1–10 (2018)